International Journal of Bio-Science and Bio-Technology
Vol.6, No.4 (2014), pp.87-98
http://dx.doi.org/10.14257/ijbsbt.2014.6.4.09

Performance Evaluation of Conventional Mixing Ventilation Systems for Operating Room in the view of Infection Control by Numerical Simulation

Sanjeev B Thool[1] and Shobha Lata Sinha[2]

Department of Mechanical Engineering
[1](Rungta College of Engineering, Bhilai, India)
sbthool@rediffmail.com
[2](National Institute of Technology, Raipur, India)
shobha_sinha1@rediffmail.com

Abstract

To reduce the possibility of post operation infection resulting from contaminant particles, effective ventilation system plays an important role. The best way to treat an infection is to stop it from occurring in the first place. Concerning the same objective, conventional mixing ventilation systems have been used since long period. Mixing room air distribution aims for dilution of polluted and warm/cool room air with cleaner and cooler/warmer supply air.

In this paper three cases of mixing ventilation systems i.e. Single-sided high supply and low exhaust (Case-1); high supply and low exhaust (Case-2) and low supply and high exhaust (Case-3) are investigated using Computation Fluid Dynamics (CFD) Technique.

It has been observed that contamination control has been found more effective in case-3 as thermal plumes plays the dominant role.

Keywords: *Mixing ventilation, Air distribution, Infection control, Operating room, Surgical site*

1. Introduction

Mixing room air distribution aims for diluting of polluted and warm/cool room air with cleaner and cooler/warmer supply air. The air is supplied to the room with high initial mean velocity and the established velocity gradients generate high turbulence intensity aiming to promote good mixing and uniform temperature and pollution distribution in the occupied zone. Mixing Ventilation is an expression for an air distribution pattern, and not for a ventilation system. It can also be called an air distribution pattern with mixing effect or mixing air distribution. Mixing ventilation is traditional considered to be the air distribution, which is obtained by the use of diffusers with high momentum supply flow.

Conventional (mixing) ventilation systems are used in old hospital's operating room, mostly in the developing countries. These systems are normally used for general surgeries such as abdominal surgery. Conventional ventilation system comprises inlet and exhaust opening on walls at different disposition with conventional mixing. Selection of air distribution schemes is critical for the whole system performance with regard to the contamination removal effectiveness. By maintaining the proper direction of airflow, proper inlet and outlet orientation, proper inlet area to wall area ratio and distribution of heat source can demonstrate the air distribution pattern can be controlled by buoyancy from heat sources. The problem associated with these systems is with maintaining laminar airflow across the critical area in operating room, especially on cooling. In order to avoid the turbulent airflow pattern to some extent in this area, an alternative method to the

ISSN: 2233-7849 IJBSBT

conventional cross flow ventilation system is analyzed and compared. This alternative system is just modeled by changing the inlet and exhaust openings of the conventional ventilation system so that airflow movement is altered.

In this paper, three types of ventilation systems modeled are analyzed by CFD simulation. These are (i) conventional one-sided high supply and low exhaust (Case-1), (ii) high supply and low exhausts (Case-2) and (iii) low supply and high exhaust (Case-3). The common thing in these systems is that inlet and exhausts opening are located on walls only and operating on acceptable range of ACH. Figure 1 shows the modeling of inlet-outlet configuration of three ventilation systems.

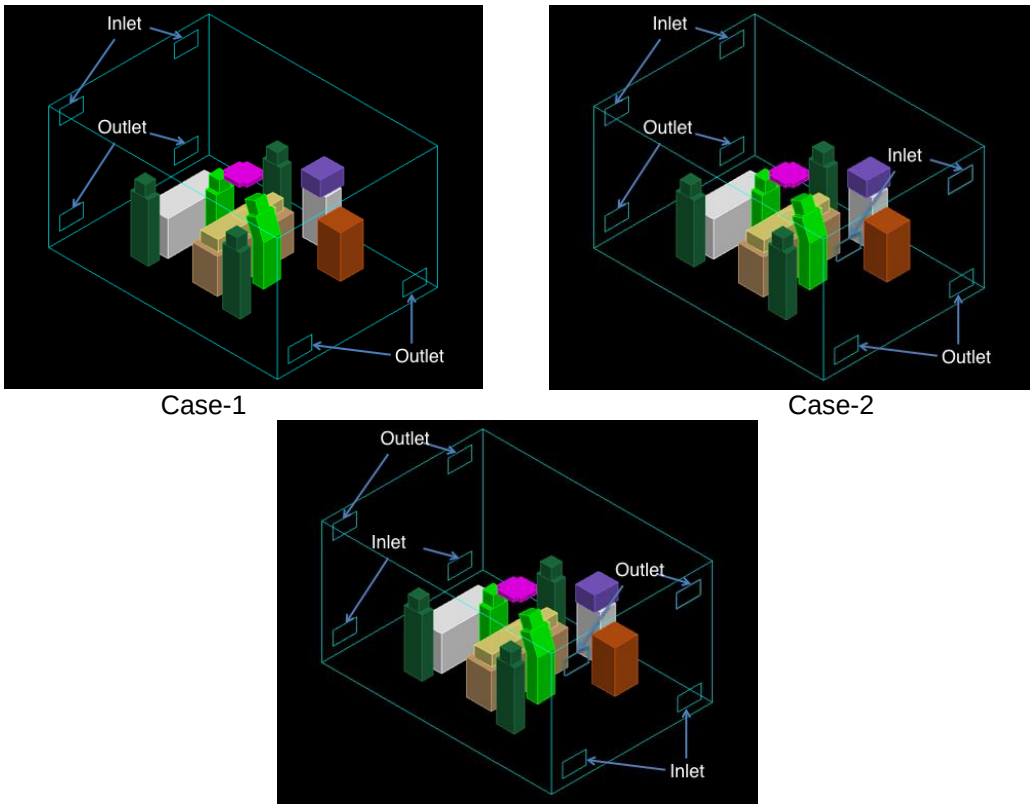

Figure 1. Mixing Ventilation Configurations

2 CFD Modeling

2.1. Governing Equations for Turbulent Flow

Airflow pattern in room is calculated by using Eulerian approach. The airflow and the heat transfer are described mathematically by a set of differential equations for mass, momentum and energy equations based on the solution of the general advection – diffusion equation:

$$\frac{\partial(\rho\phi)}{\partial t}+\frac{\partial(\rho\vec{V}\phi)}{\partial x}+\frac{\partial(\rho\vec{V}\phi)}{\partial y}+\frac{\partial(\rho\vec{V}\phi)}{\partial z}=\frac{\partial}{\partial x}\left[\Gamma_\phi\frac{\partial\phi}{\partial x}\right]+\frac{\partial}{\partial y}\left[\Gamma_\phi\frac{\partial\phi}{\partial y}\right]+\frac{\partial}{\partial z}\left[\Gamma_\phi\frac{\partial\phi}{\partial z}\right]+S_\phi \qquad (1)$$

where, ϕ represents the independent variables: time averaged velocity components *V (i.e. u, v, w)*, turbulent kinetic energy, *k*, dissipation rate of turbulent kinetic energy, ε, and enthalpy *H*. When ϕ is unity, the equation represents the conservation of mass.

Expressions for the effective diffusivity, Γ_ϕ and source term, S_ϕ for each variable and the corresponding empirical numbers are described by Launder and Spalding (1972) [1].

In order to model the random feature of turbulent flows, a time decomposition (also called Reynolds decomposition) of the instantaneous flow variables $\phi(t)$ is introduced into the governing flows.

$$\phi(t) = \bar{\phi} + \phi'(t) \quad (2)$$

The mean value of $\phi(t)$ is obtained by integrating $\phi(t)$ over a period of time dt that is much longer than the fluctuating duration:

$$\bar{\phi} = \frac{1}{\tau}\int_t^{t+dt} \phi(t_1)\, dt_1 \quad (3)$$

Algebraic expressions of generic equation (Eq. 3.1) for various transport properties are formulated and hereafter solved. By setting the transport property ϕ equal to 1, u, v, w, T, k, ε, and selecting appropriate values for the diffusion coefficient Γ_ϕ and source terms S_ϕ, we obtain the special forms presented in Table 1 for each of the partial differential equations for the conservation of mass momentum, energy, and the turbulent quantities.

Table 1. General Expression of ϕ, Γ_ϕ and S_ϕ for Various Conservation Equations for Incompressible Flow in Cartesian Coordinates

Equations	ϕ	Γ_ϕ	S_ϕ
Continuity	*1*	*0*	0
u-momentum	u	$\nu + \nu_T$	$-\frac{1}{\rho}\frac{\partial p}{\partial x} + S'_u$
v-momentum	v	$\nu + \nu_T$	$-\frac{1}{\rho}\frac{\partial p}{\partial y} + \frac{T}{\rho}\frac{Gr}{Re^2} + S'_v$
w-momentum	w	$\nu + \nu_T$	$-\frac{1}{\rho}\frac{\partial p}{\partial z} + S'_w$
Temperature	T	$\frac{\nu}{Pr} + \frac{\nu_T}{Pr_T}$	S_T
Turbulent kinetic energy	k	$\frac{\nu_T}{\sigma_k}$	$P - D + G_{buoy}$
Energy dissipation rate	ε	$\frac{\nu_T}{\sigma_\varepsilon}$	$\frac{\varepsilon}{k}(C_{\varepsilon 1}P - C_{\varepsilon 2}D) + \frac{\varepsilon}{k}C_{\varepsilon 1}C_{\varepsilon 3}\, max(G_{buoy}, 0)$

Additional source terms in the momentum equations S'_u, S'_v, and S'_w comprise of the pressure and nonpressure gradient terms and other possible sources such as gravity that influence the fluid motion, whereas the additional source term S_T in the energy equation may contain heat sources or sinks within the flow domain.

where,

$$P = 2\nu_T\left[\left(\frac{\partial u}{\partial x}\right)^2 + \left(\frac{\partial v}{\partial y}\right)^2 + \left(\frac{\partial w}{\partial z}\right)^2\right] + \nu_T\left[\left(\frac{\partial u}{\partial y} + \frac{\partial v}{\partial x}\right)^2 + \left(\frac{\partial v}{\partial z} + \frac{\partial w}{\partial y}\right)^2 + \left(\frac{\partial w}{\partial x} + \frac{\partial u}{\partial z}\right)^2\right];$$

$D = \varepsilon$; and

$$G_{buoy} = g\frac{\mu_T}{\sigma_T}\frac{1}{\rho}\frac{\partial p}{\partial y}$$

$\sigma_k = 1.0$; $\sigma_\varepsilon = 1.3$; $C_{\varepsilon 1} = 1.44$; $C_{\varepsilon 2} = 1.92$; $C_{\varepsilon 3} = 1.0$.

2.2. Equations for Particle Motion and Dynamics

Particle motion in carrier fluid is affected by various forces such as viscous drag force, gravity force, added mass force (virtual mass force), Brownian force, and pressure force. In this study, Brownian force has been ignored due to the large size of particle. The added mass force was considered in a few simulations and was found to have negligible influence on particle trajectory [2]. Thus in this study, steady viscous drag force, gravity force and pressure force have been considered.

The methodology for predicting turbulent particle dispersion used in this study is originally laid out by Gosman and Ioammides [3] and validated by Ormancey and Martinon [4]. Turbulence was incorporated into the *stochastic* model via the *k–ε* turbulence model (Alani *et al*.) [5].

The Lagrangian particle tracking method is used to calculate individual trajectories by solving the momentum equation. By equating the particle inertia with external forces, the momentum equations can be expressed as:

$$m_p \frac{du_p}{dt} = \frac{1}{2} C_D A_p \rho (u - u_p) \sqrt{(u - u_p)^2 + (v - v_p)^2 + (w - w_p)^2} + m_p g_x \quad (4)$$

$$m_p \frac{dv_p}{dt} = \frac{1}{2} C_D A_p \rho (v - v_p) \sqrt{(u - u_p)^2 + (v - v_p)^2 + (w - w_p)^2} + m_p g_y \quad (5)$$

$$m_p \frac{dw_p}{dt} = \frac{1}{2} C_D A_p \rho (w - w_p) \sqrt{(u - u_p)^2 + (v - v_p)^2 + (w - w_p)^2} + m_p g_z \quad (6)$$

where

$$C_D = \frac{24}{Re}\left(1 + \frac{3}{16} Re\right)^{0.5} \quad \text{for } Re \leq 560; \quad (7)$$

and

$C_D = 0.44$ …. for $Re > 560$

The Reynolds number of the particle is based on the relative velocity between particle and air.

In laminar flow, particles released from a point source with the same weight would initially follow the airstream in the same path and then fall under the effect of gravity. Unlike laminar flow, the random nature of turbulence indicates that the particles released from the same point source will be randomly affected by turbulent eddies. As a result, it will be diffused away from the streamline at different fluctuating levels. In order to model the turbulent diffusion, the instantaneous fluid velocities in the three Cartesian directions u, v and w are decomposed into the mean velocity component and the turbulent fluctuating component as:

$$u = \bar{u} + u'; \qquad v = \bar{v} + v'; \qquad w = \bar{w} + w'$$

where, $\bar{u}$ and *u'* are the mean and fluctuating components of velocity in *x* – direction. The same applies for *y* and *z* directions. The stochastic approach prescribes the use of a random number generator algorithm, which, in this case, is taken from Press *et al*. [6] to model the fluctuating velocity. It is achieved by using a random sampling of a Gaussian distribution with a mean of zero and a standard deviation of unity. Assuming isotropic

turbulence, the instantaneous velocity of air are then calculated from kinetic energy of turbulence:

$u = \bar{u} + N\alpha$; $v = \bar{v} + N\alpha$; $w = \bar{w} + N\alpha$.

where *N* is the pseudo-random number, ranging from 0 to 1, with

$$\alpha = \left(\frac{2k}{3}\right)^{0.5} \quad (8)$$

The mean velocity, which are the direct output of CFD, determine the convection of the particles along the streamline, while the turbulent fluctuating velocity, $N\alpha$, contributes to the turbulent diffusion of the particle.

3. Brief of Operating Room

In a typical operating room layout five surgical staff member, lights, machinery, tables and patient are considered for the baseline model for the CFD simulations. The brief description of operating room is given in the Table 1. The size of each inlet and exhaust grille is 0.61 m x 0.36 m. The most suitable operating value of ACH for this system is ranging from 20 h^{-1} to 25 h^{-1} [7]. The present CFD simulation is done taking ACH as 25 h^{-1} and air velocity as 0.64 m/s with temperature as 27 ℃.

Table 2. Dimensions and Heat Dissipation of Major Items in Operating Room

Item	Dimensions	Heat Dissipation	Heat Flux
Operating table	0.64 m x 2.0 m x 0.9 m	None	--
Surgical lamp	0.55 m x 0.55 m x 0.1 m	150 W	182 W/m^2
Anesthesia machine	0.6 m x 0.6 m x 1.1 m	200 W	76 W/m^2
Back table	0.64 m x 1.6 m x 0.9 m	None	--
Monitor stand	0.6 m x 0.5 m x 1.20 m	None	--
Monitor	0.5 m x 0.4 m x 0.6 m	200 W	185 W/m^2
Surgical staff (Two surgeon and three nurses)	0.46 m x 0.28 m x 1.8 m each	100 W each	37 W/m^2 each
Patient	0.46 m x 0.28 m x 1.8 m	Exposed head dissipates 46 W. Surgery site (0.3 m x 0.3 m) area with surface temperature = 38 ˚C	--

4. Boundary and Initial Conditions

The velocity, temperature and turbulent transport quantities over the inlet boundary are prescribed from the experimental data found by Memarzadeh and Manning [7]. Outlet boundary conditions are set as the Neumann boundary condition. No slip boundary condition has been used at the wall. Wall functions are applied to describe the turbulent flow properties in the near wall reason.

The initial conditions for particle tracking include the starting position and initial velocities of particles. For this study, the particles are assumed as skin flakes (or squames) generated from the exposed skin (forehead) of the surgical staff having the density of ρ_p = 850 kg/m^3. Particles are equally divided into three size groups of 10, 15 and 20 microns.

The representative number of particles generated is taken as 576 for 1 hour of surgery. Other boundary conditions regarding the rate of generation of contaminant particles, heat generation from equipment and human bodies are illustrated in Table 2.

When particles reach exhaust outlets, they will escape and the trajectories terminate. When reaching a rigid object, particles may either attach to or rebound from the object's surface. Particles in a ventilated room are most likely to attach to the surface since they usually cannot accumulate enough rebound energy to overcome adhesion [8]. It is therefore natural to terminate, or "trap", a particle trajectory after hitting a rigid surface. This treatment was adopted and used in many CFD studies of the indoor environment.

Nevertheless, the trap treatment worked well when the near-wall grid was sufficiently fine, like that which was used in the Direct Numerical Simulation (DNS) (McLaughlin; Narayanan *et al.*) [9, 10]. The trap treatment, however, is not suitable for the current situation, which uses a high Reynolds number k-ε model. Instead of using trap treatment, this study set the restitution coefficient to a very small value. By doing so, particles were immediately stopped without being trapped after reaching a surface. When particles acquired sufficient normal velocity, they escaped from the boundary layer and became re-suspended. This implies that deposition is neglected. Such manipulation may only be suitable when particle deposition rate is very low.

5. Particle Tracking

The methodology is refined to consider different particle outcomes, namely:

- The particle is vented from the room via ventilation and
- The particle hits one of the two designated targets, namely, the surgical site (patient body put under surgery) or the top surface of the back table.

Particles that are neither vented nor strike the target are assumed to remain in the room when the overall particle tracking time limit (1 hour in present case) is reached.

6. Results of Numerical Simulation

The numerical simulation is carried out for ACH of 25 h^{-1}. Figure 2 shows the numerical simulation results obtained by FLUENT software [11]. In Case-1, streamline contours (Figure 2 a) clearly shows that air is flowing over the critical area crossing the back table, two nurses and supporting surgeon. Due to these obstacles, velocity of air is attenuated and particles may not be able to escape without striking on the surgical site. Velocity distribution (Figure 2 b) shows the major recirculation flow zones are created on both sides of critical space of operating room. One recirculation zone, just above the floor covering inlet diffuser side of operating room has been observed. This zone captures the area around the back table where stagnation of air is more as compared to other zone. Similarly one recirculation at middle of the operating room above the operating table has also been observed. Velocity contours (Figure 2 c) shows that there is a formation of stagnant region between the main surgeon and patient, which may cause the trapping of particles generated by the surgeons.

In Case-2, streamline contours (Figure 3 a) and velocity distribution (Figure 3 b) clearly show that only curvature downward movement of airflow and recirculation zones at the four corners of the operating room which may cause the relatively heavy particles (20 μm) strike on back table and surgical site. It has been also observed from velocity distribution (Fig. 3 c) that a recirculation zones are formed on both sides of the patient between two surgeons performing surgery. This causes the possibility of trapping of particles generated by surgeons in this region.

In Case-3, streamline contours (Figure 4 a) show that there in no airflow crossing the critical space around the operation table. Only upward curvature movement of airflow is created at four corners of operating room. It is also observed from the velocity vector

(Figure 4 b) that vertical upward velocity vectors above the patient that is due to the both upward momentum and thermal plumes induced by the surgical site. These thermal plumes are experienced due to the fact that there is no counteracting effect of horizontal velocity due to ventilation system on the convective flow of air due to relatively higher temperature of surgical site lamp. The airflow above the surgical site in upward direction supplemented by thermal plume drives the small particles up to the high level of exhausts. It has been also observed from velocity contours (Figrue 4 c) that a recirculation zones are formed on both sides of the patient between two surgeons performing surgery. This causes the possibility of trapping of relatively heavier particles generated by surgeons in this region.

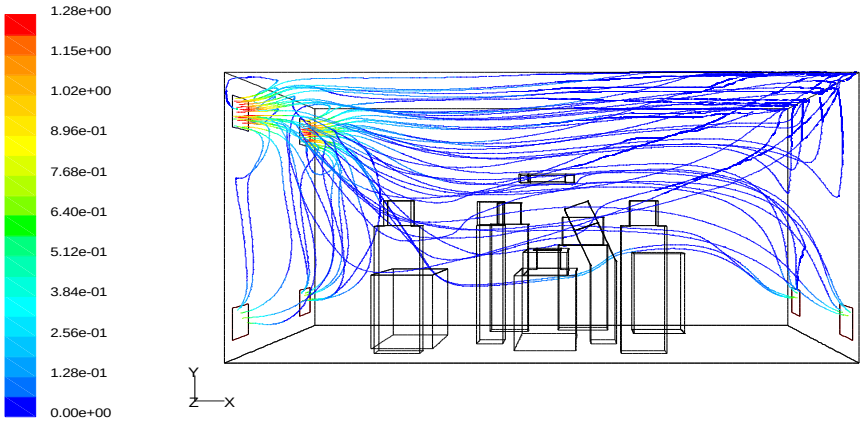

(a) Streamline Contours

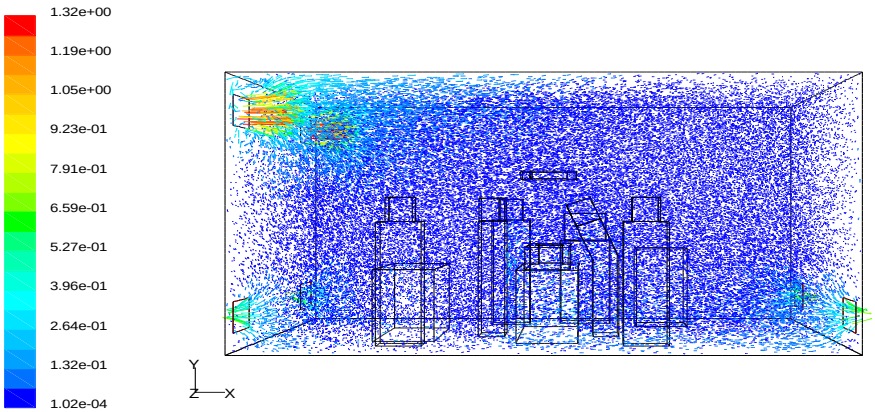

(b) Velocity distribution

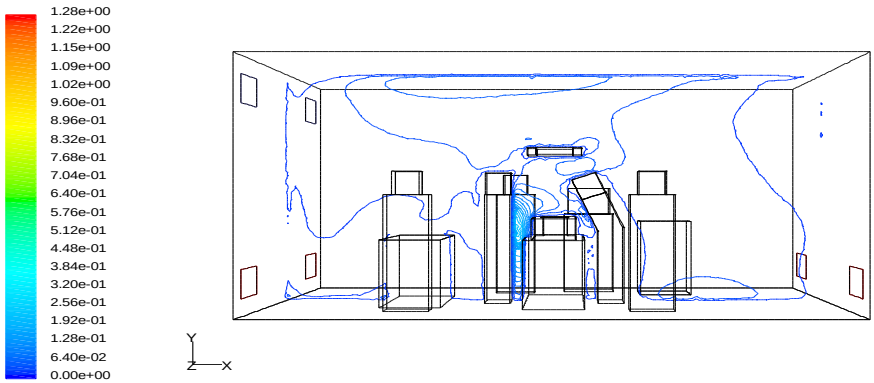

(c) Velocity contours (at plane at z = 0)

Figure 2. Numerical Simulation of Case-1

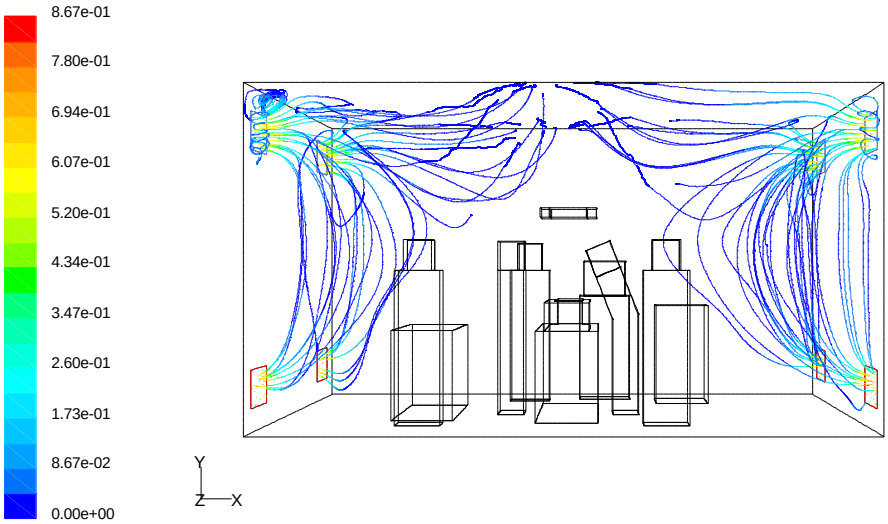

(a) Streamline Contours

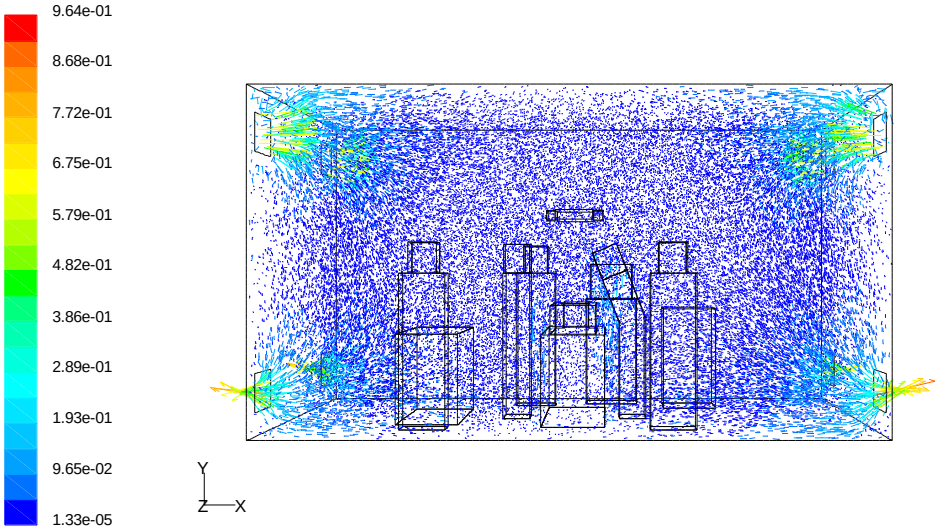

(b) Velocity Distribution

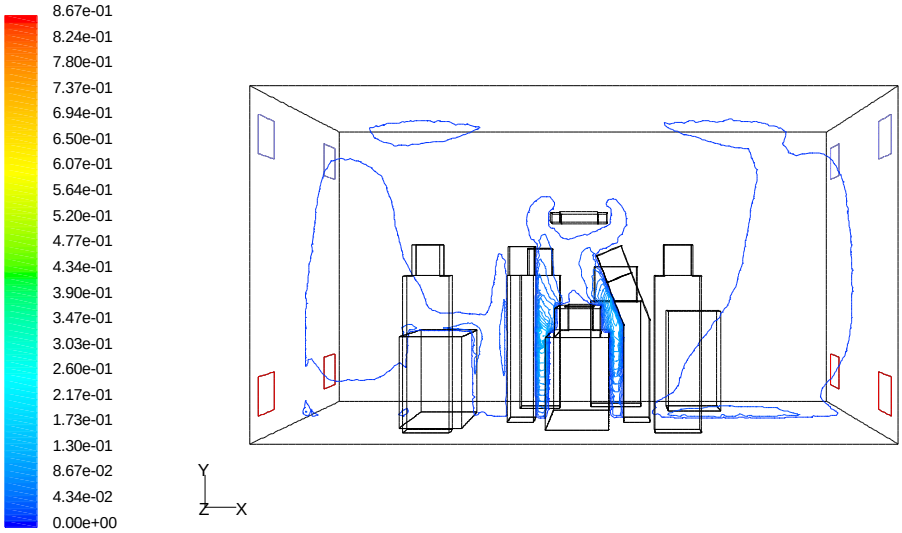

(c) Velocity Contours (at vertical plane at z = 0)

Figure 3. Numerical Simulation of Case-2

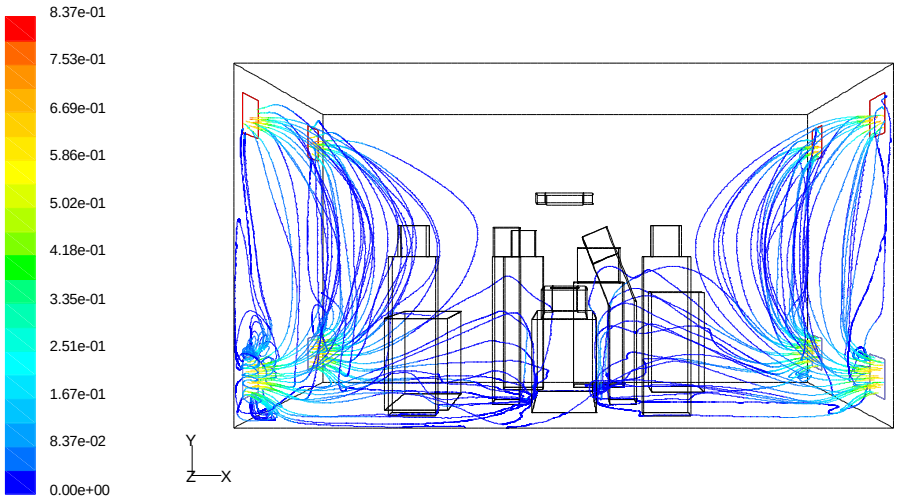

(a) Streamline Contours

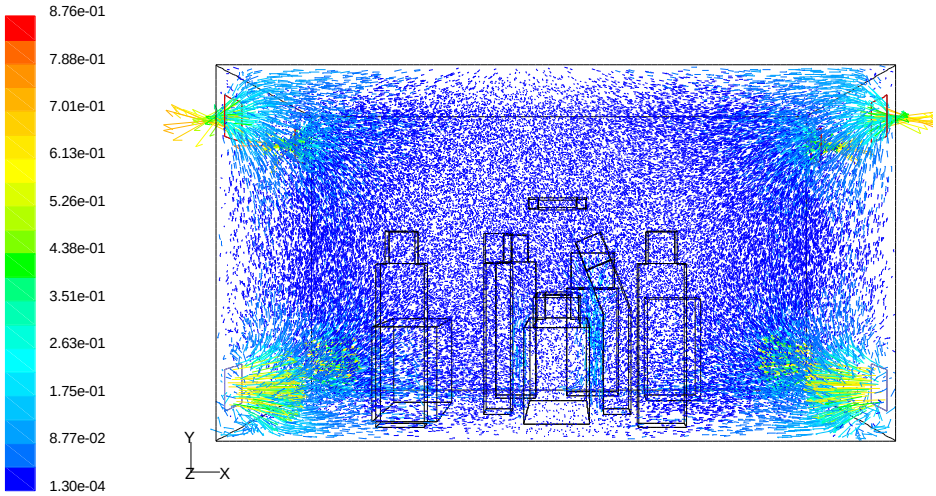

(b) Velocity distribution

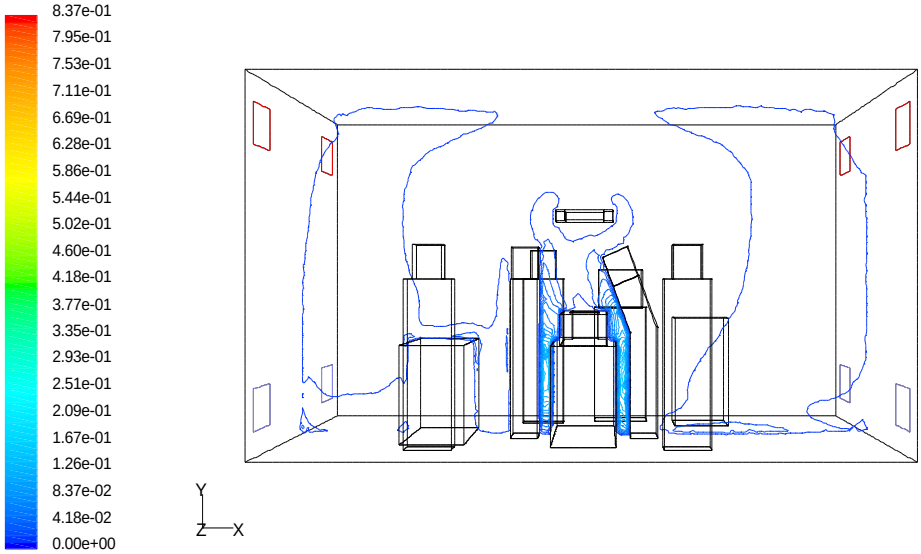

(c) Velocity contours (at vertical plane at z = 0)

Figure 4. Numerical Simulation of Case-3

7. Particle Trajectory Simulation and Performance Discussion

In these systems, the air moves across contaminated personnel and equipment before reaching the patient, resulting in localized areas of turbulent flow and low velocity recirculation zones, thus possibly increase the risk of infection. There are the problems associated with maintaining laminar airflow across the entire room, especially on cooling.

The predominant design factor for these systems is quantity of supply air. This is determined by considering both the required air change rate and space cooling loads. The air change rate is often detrimental. Air Change per Hour (ACH) is the time rate at which the room air is replaced based on total supply air quantity into the space and room volume.

Results from the numerical simulation (Table 3 - 4) show the effectiveness of these three cases in removing the particles via ventilation. This is an expected result, but there are some interesting points drawn from the results. For same ACH, there is a marked difference in terms of the percentage of particles removed via ventilation. Case-3 (Table 3) demonstrates better performance in removing the tiny sized particles (10 and 15 μm) from the operating room, even better results demonstrated for particle size of 10 μm. The overall percentage of particles strikes on surgical site (0.12%) and back table (0.61%) is also small compared to the others. Case-1 and Case-2 demonstrate nearly same performance in terms of contaminated particles strikes on surgical site and back table. There is no noticeable difference between the performances of Case-1 and Case-2 systems in terms of percentage of particles removed from the operating room for particle size of 20 μm. But Case-2 demonstrates better performance as compared to Case-1 in terms of total number of particles of size 10 μm and 15 μm, escaped from the operating room. Case-3 ventilation system works with the thermal plume in the center of the room in driving the particles up to the high level exhausts.

However, it is verified that this performance is affected by the heat load in the operating room, which in turn is affected by the amount and type of equipment, people and lights used. Other variable may also affect the efficiency, for example the movement of people in the operating room, and the occurrence of open doors.

Table 3. Percentage of Particles Vented from Room and Percentage of Particles Strike on Surgical Site and Back Table for Case-1

Particle Size (μm)	Particle Source	Total Number of particles released	Contaminated particles (Skin flakes) escaped from Operating Room		Contaminated Particles (Skin flakes) Strike on Surgical Site		Contaminated Particles (Skin flakes) Strike on Back Table	
			Nos	%	Nos	%	Nos	%
10	Surgeons	192*2 = 384	304	79.1	0	0.0	1	0.26
	Nurses	192*3 = 576	485	82.2	1	0.17	6	1.0
15	Surgeons	192*2 = 384	307	80	1	0.26	2	0.52
	Nurses	192*3 = 576	482	83.7	0	0.0	8	1.4
20	Surgeons	192*2 = 384	285	74.2	1	0.26	4	1.0
	Nurses	192*3 = 576	427	74.1	2	0.35	11	1.9
Average %				**78.88**		**0.17**		**0.98**

Table 4. Percentage of Particles Vented from Room and Percentage of Particles Strike on Surgical Site and Back Table for Case-2

Particle Size (μm)	Particle Source	Total Number of particles released	Contaminated particles (Skin flakes) escaped from Operating Room	Contaminated Particles (Skin flakes) Strike on Surgical Site	Contaminated Particles (Skin flakes) Strike on Back Table

			Nos	%	Nos	%	Nos	%
10	Surgeons	192*2 = 384	330	85.9	0	0.0	1	0.26
	Nurses	192*3 = 576	516	89.6	1	0.17	6	1.0
15	Surgeons	192*2 = 384	309	80.5	0	0.0	2	0.52
	Nurses	192*3 = 576	491	85.2	1	0.17	6	1.0
20	Surgeons	192*2 = 384	281	73.2	1	0.26	2	0.52
	Nurses	192*3 = 576	436	75.7	2	0.35	6	1.0
Average %				**81.68**		**0.16**		**0.72**

Table 5. Percentage of Particles Vented from Room and Percentage of Particles Strike on Surgical Site and Back Table for Case-3

Particle Size (μm)	Particle Source	Total Number of particles released	Contaminated particles (Skin flakes) escaped from Operating Room		Contaminated Particles (Skin flakes) Strike on Surgical Site		Contaminated Particles (Skin flakes) Strike on Back Table	
			Nos	%	Nos	%	Nos	%
10	Surgeons	192*2 = 384	338	88.2	0	0.0	0	0.0
	Nurses	192*3 = 576	517	89.8	0	0.0	0	0.0
15	Surgeons	192*2 = 384	310	80.7	0	0.0	1	0.26
	Nurses	192*3 = 576	490	85.1	0	0.0	6	1.0
20	Surgeons	192*2 = 384	280	72.9	2	0.52	4	1.0
	Nurses	192*3 = 576	402	69.8	1	0.17	8	1.4
Average %				**81.08**		**0.12**		**0.61**

8. Conclusion

Conventional ventilation system in operating room is having inlet and outlet located at opposite walls only with relatively high air velocity at inlet causing turbulence in the room. Three types of ventilation system under this category is investigated that is single-sided high supply and low exhaust (Case-1); high supply and low exhaust (Case-2); and low supply and high exhaust (Case-3). An interesting interaction between air distribution, recirculation zone, airflow pattern, buoyancy effect and particle trajectory has been observed in this investigation. For the same ACH these systems show marked differences in terms of the percentage of particles removed via ventilation. Case-3 demonstrates better performance than other two cases in terms of number of particles strike on surgical site and back table. This is because of Case-1 results in the formation of two large recirculation in the room where particles can become trapped. In Case-2, curvature downward movements of airflow zones are created at four corners of operating room. It has also been observed in simulation results that in Case-1 stagnant region is formed in the space between the main surgeon and patient, which cause to trap the particles on the surgical site.

Particle trajectory simulation results also show that percentage of tiny particles (10 and 15 μm) trapped on back table and surgical site in case-3 is also less as compared to that occurred in Case-1 and Case-2. This is because of in Case-3 area above the surgical site experience effect of thermal plume induced by relatively high temperature of surgical site and lamp. This causes the vertical upward flow of air that opposing the light contaminated particle to get trapped on the surgical site.

NOMENCLATURES

Symbol	**Description**
C_D	Drag coefficient;

Dt	Time interval;
G	Gravitational acceleration;
k	Turbulent kinetic energy;
N	Pseudo-random number;
T	Temperature;
t	Time;
Pr	Prandtl number;
S_ϕ	Source term in governing equation;
$\vec{V}$	Velocity;
u, v, w	Velocity components of air in x, y and z directions;
A_p	Cross-sectional area of the particle;
m_p	Mass of particle.

Greek Symbols

Γ_ϕ	Effective diffusivity;
ε	Turbulent kinetic energy dissipation rate;
α	Thermal diffusivity ($k/\rho c_p$);
μ	Dynamic viscosity;
ν	Kinematic viscosity (μ/ρ);
ν_T	Turbulent kinematic viscosity;
ρ	Mass density;
σ_T	Stress due to turbulent flow.

Superscripts

-	Time-averaged value;
’	Fluctuating value.

Subscripts

x, y, z	Abscissa and ordinate of rectangular Cartesian; coordinate system;
P	Particle;
T	Turbulent flow.

References

[1] B. E. Launder, D. B. Spalding, Lectures in Mathematical Models of Turbulence. Academic Press, London, England, (1972).
[2] S. L. Sinha, R. C. Arora, and Subhransu Roy, Numerical Simulation of Two Dimensional Room Air Flow with and Without Buoyancy, Energy And Buildings, 32(1), pp. 121–129 (2000).
[3] D. Gosman and E. Ioannide, Aspect of computer simulation of liquid-fuelled combustion. AIAA 19th Aerospace Science Meeting 81-0323, 1 – 10, (1998).
[4] Ormancey and J. Martinon, Prediction of particle dispersion in turbulent flow, Physico Chemical Hydrodynamics, 5, 229 – 224, (1984).
[5] A. Alani D. Dixon-Hardy and M. Seymour, Contaminants transport modeling. EngD in Environmental Technology Conference, (1984).
[6] W. H. Press, S. A. Teukolsky, W.T. Vetterling and B. P. Flannary, Numerical recipes in FORTRAN, 2d ed. Cambridge, Cambridge University Press, (1992).
[7] Farhad Memarzadeh, Andrew P. Manning, Comparison of Operating Room Ventilation Systems in the Protection of the Surgical Site.
[8] W. C. Hinds, Aerosol Technology, Properties, Behavior, and Measurement of Airborne Particles. Wiley, New York, (1982).
[9] McLaughlin JB, Aerosol particle deposition in numerically simulated channel flow, Physics of Fluids A 1 (7), 1211–1224, (1989).
[10] C. Narayanan, D. Lakehal, L. Botto, A. Soldati, Mechanisms of particle deposition in a fully developed turbulent open channel flow. Physics of Fluids 15 (3), 763–775, (2003).
[11] FLUENT, Fluent 6.2 User’s guide. Fluent Inc., Lebanon, NH, (2005).

